



## Direct Shear Tests on Soft Clay Reinforced with Single Ordinary Granular Column: Discrete Element-Finite Difference Method

M. Hazeghian\*

Department of Civil Engineering, Yazd University, Yazd, Iran

### PAPER INFO

#### Paper history:

Received 28 February 2024

Received in revised form 30 March 2024

Accepted 04 April 2024

#### Keywords:

Soil Improvement

Soft Clay Soil

Ordinary Granular Column

Discrete Element Method

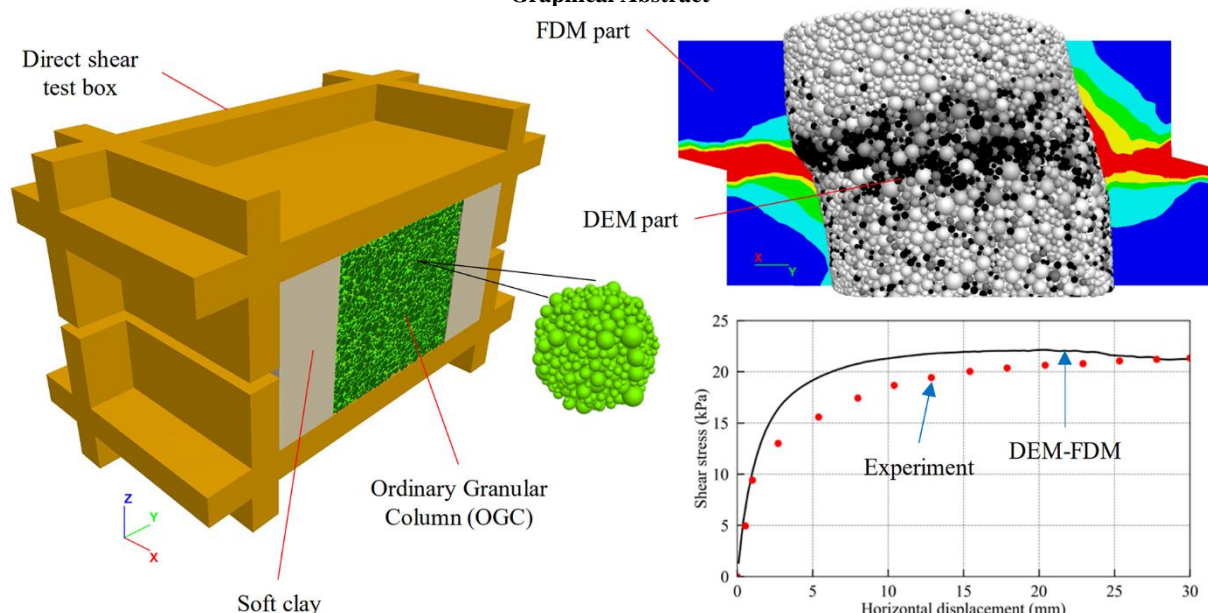
Direct Shear Test

### ABSTRACT

A great deal of research has been conducted on the performance of granular columns under vertical loads. However, in some situations, the movement of the soil mass can lead to lateral deformations and, as a result, shear stresses in the soil and columns. The primary objective of the present study is to numerically investigate the shear performance of soft clay soil improved with a single Ordinary Granular Column (OGC) in the direct shear test using a hybrid Discrete Element-Finite Difference Method (DEM-FDM). The numerical modeling method was first validated by simulating a direct shear test conducted previously on a soft clay-OGC composite in the laboratory. Afterward, an extensive parametric study was conducted to determine how various factors affect the shear strength of clay-OGC composites. According to the results, increasing the area replacement ratio from 15 to 35% can increase the peak shear strength of clay-OGC composites in the direct shear test by up to two times, depending on the level of applied normal stress. The micro-scale results also indicated that the surface roughness of soil particles in OGC has a greater effect on the shear strength of clay-OGC composites than their angularity. Furthermore, the results showed that the equivalent friction angle of clay-OGC composites should be calculated based on the residual friction angle of granular soil used in OGC.

doi: 10.5829/ije.2024.37.09c.09

### Graphical Abstract



\*Corresponding author Email: [m.hazeghian@yazd.ac.ir](mailto:m.hazeghian@yazd.ac.ir) (M. Hazeghian)

Please cite this article as: Hazeghian M. Direct Shear Tests on Soft Clay Reinforced with Single Ordinary Granular Column: Discrete Element-Finite Difference Method. International Journal of Engineering, Transactions C: Aspects. 2024;37(06):1790-9.

## 1. INTRODUCTION

There are many infrastructure projects (railways, highways, etc.) constructed on sites with serious geotechnical concerns. As a result, ground improvement is of utmost importance in these projects. There are several techniques available to improve the ground, including preloading, compaction, rigid piles, granular columns, etc. (1).

Granular columns have been used extensively to increase the bearing capacity of the soil under foundations and embankments, reduce total and differential settlement, speed up consolidation settlement, reduce the risk of liquefaction, and enhance slope stability. Typically, granular columns are used to increase load capacity and are subjected to vertical loads. For this reason, numerous studies have been conducted to better understand their behavior under vertical loads (2-6). However, in certain instances, the performance of granular columns under lateral loading is of special significance. An example would be granular columns used to maintain slope stability or below the toe of embankments.

Compared to vertical loads, the behavior of granular columns under shear has received less attention in the past (7). A series of direct shear tests was conducted by Aslani, Nazariafshar (8) to investigate the shear behavior of granular columns in soft clay soils. Several factors were considered in this study, including the amount of applied stress, the area replacement ratio, as well as the type of material used in granular columns. Specifically, they demonstrated that area replacement ratios greater than 15% are associated with a significant rate of increase in shear strength. Murugesan and Rajagopal (9) performed several large-scale direct shear tests to compare the behavior of Ordinary Granular Columns (OGC) and Encased Granular Columns (EGC) under shear loading, finding that EGCs exhibit significantly higher shear resistance than OGCs.

Numerical analyses have been widely employed to improve our understanding of the behavior of stone columns. Numerical methods based on continuum mechanics, such as Finite Element Method (FEM) and Finite Difference Method (FDM), have been extensively used to study stone columns previously (2, 10-13). However, due to the problems that these numerical methods have in modeling stone columns and their interaction with the surrounding soil, many researchers in the past have utilized combined DEM-FEM and DEM-FDM methods (14-18). In these hybrid approaches, stone columns are modeled using DEM and the surrounding soil is modeled using FEM or FDM.

The majority of numerical studies have been conducted on the behavior of stone columns under vertical loads; less attention has been paid to their performance under shear loads. For the purpose of

understanding the shear load-bearing capacity of OGC and EGC granular columns, Mohapatra, Rajagopal (19) performed a series of 3D numerical simulations using FLAC3D software. The shear stresses mobilized within the granular columns of EGC were higher than those mobilized within the columns of OGC. Further, it was found that both circumferential and vertical tensile forces are mobilized within the geosynthetic encasement, which contributes to the increased shear strength of the granular column.

A comprehensive review of past research revealed that no numerical study of the shear behavior of granular columns has been conducted using the combined DEM-FDM method. Accordingly, the present study aims to numerically model the shear behavior of a single ordinary granular column used for improving soft clay in a large-scale direct shear test using this hybrid method.

The present study is structured as follows. Firstly, the micro parameters used in the modeling are calibrated by simulating a large-scale direct shear test that was previously performed by Aslani, Nazariafshar (8). Then, the impact of various parameters on the shear strength of the isolated granular column, at the macro scale, such as the level of applied stress, column diameter, and relative density of the granular column, and at the micro-scale, such as the roughness and shape of grains, is evaluated within the framework of an extensive parametric study.

## 2. RESEARCH METHOD

This section begins with a summary of DEM and DEM-FDM formulations. A numerical methodology is then presented for modeling the shear behavior of a single granular column in soft clay soil during a Direct Shear Test (DST). In the following, micro parameters are calibrated based on the results of a laboratory DST test. Finally, a description of the program of DEM tests for parametric analysis is provided.

### 2. 1. DEM Formulation and DEM-FDM Coupling

The Discrete Element Method (DEM) is a numerical method for computing the motion and effect of particles. This method originated by Cundall and Strack (20) in geotechnical engineering. It is widely used nowadays for modeling and understanding soil behavior, particularly on a micro-scale.

In the present study, simulations were conducted using the PFC3D software (21). The rolling resistance linear model was employed to calculate contact interactions. In this model, particle shape can be simulated to some extent by considering the rolling resistance between spherical particles. According to this model, the normal ( $\vec{F}_n$ ) and shear ( $\vec{F}_s$ ) contact forces, as well as the rolling moment ( $\vec{M}_r$ ) between particles, are

calculated using Equations 1 to 3.

$$\vec{F}_n = k_n U_n \vec{n} \quad (1)$$

$$\vec{F}_s = \vec{F}_s + k_s \Delta \vec{U}_s, \quad \|\vec{F}_s\| \leq \mu \|\vec{F}_n\| \quad (2)$$

$$\vec{M}_r = \vec{M}_r + k_r \Delta \vec{\theta}_r, \quad \|\vec{M}_r\| \leq \mu_r \bar{R} \|\vec{F}_n\| \quad (3)$$

where  $\vec{n}$ ,  $U_n$ ,  $\Delta \vec{U}_s$  and  $\Delta \vec{\theta}_r$  represent respectively the branch vector, penetration depth, incremental tangential displacement and angular increment rotation between elements and  $\bar{R}$  is the contact effective radius (21).  $\bar{R}$  is defined as:

$$\frac{2}{\bar{R}} = \frac{1}{R_1} + \frac{1}{R_2} \quad (4)$$

$R_1$  and  $R_2$  represent the radii of the end (1) and end (2) of the contact, respectively. The  $k_n$ ,  $k_s$  and  $k_r$  are the normal, shear and rolling stiffnesses at contacts, respectively. Moreover, the  $\mu$  and  $\mu_r$  are respectively the sliding and rolling friction coefficients at contacts. The  $k_s$  and  $k_r$  are computed from Equations 5 to 6, where  $\nu$  is Poisson's ratio of grains assumed to be 0.20. The damping coefficient ranges from 0 to 1, which in the present study was presumed to be 0.1.

$$k_s = \frac{2(1-\nu)}{2-\nu} k_n \quad (5)$$

$$k_r = k_s \bar{R}^2 \quad (6)$$

PFC3D software can be used in conjunction with FLAC3D software to create a DEM-FDM coupling. To establish this coupling, interface facets are attached to the faces of the elements at the boundary between the continuous and discrete domains. These facets interact with the particles of the DEM environment and are moved by contact forces during the calculation process. The displacements are transferred to the boundary elements and the strains and stresses are updated in the FDM environment. Please refer to the PFC3D software manual (21) for more information on DEM formulations and DEM-FDM coupling.

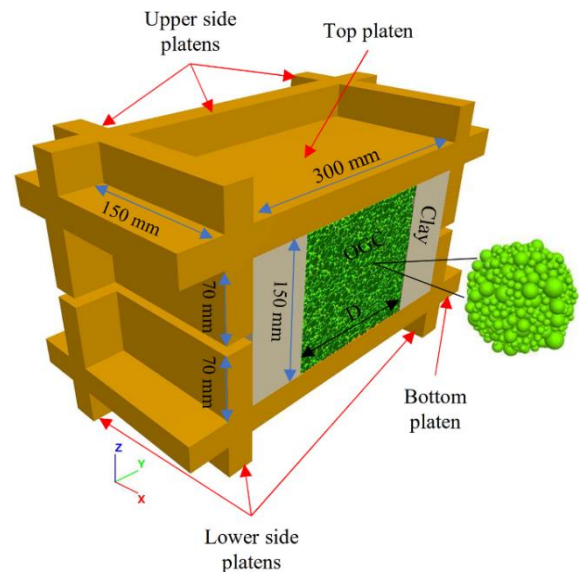
**2. 2. Numerical Modelling Methodology** This subsection describes the details and assumptions used for the numerical modeling of the Direct Shear Test (DST) on a sample of soft clay soil enhanced with a single ordinary granular column (OGC).

Figure 1 shows a three-dimensional view of half of the DST model. The upper box consists of the top platen and four side platens, and the lower box contains the bottom platen and four side platens. The platens were

modeled using rigid blocks (21). The top and bottom platens were assumed to have rough surfaces with a coefficient of friction of 1. However, it was presumed that the side platens surfaces would be smooth with a coefficient of friction of 0.2. These assumptions were considered previously by Yan and Ji (22). Moreover, It was assumed that the inner dimensions of the box would be 300×300×150 mm. The upper and lower boxes were separated by a 10 mm gap to allow the lower part of the model to move freely in relation to the upper part. A similar assumption was previously made by Potts, Dounias (23).

The soft clay sample was considered to be a continuum medium following the Mohr-Coulomb constitutive model (FDM part). The mesh grid for the clay sample consisted of tetrahedral elements with an average dimension of 10 mm. A single OGC was constructed by embedding a cylindrical space with a diameter D in the middle of the clay sample and filling it with granular soil particles (DEM part). Figure 2 shows the particle size distribution (PSD) used for the OGC, which is similar to that used by Aslani, Nazariafshar (8) for their laboratory experiments. Particles were assumed to be spherical in shape. In accordance with the method proposed by Yunjia and Erxiang (24), employing artificial interparticle friction coefficients of 0 and 5 during sample preparation, it was determined that the minimum and maximum void ratios were 0.527 and 0.685 for the assumed PSD.

Following are the steps involved in simulating the DST test on a clay sample improved with a single OGC. Initially, the test box and clay soil sample were constructed. Afterward, based on the volume of the OGC, the PSD curve and the relative density ( $D_r$ ) required for



**Figure 1.** Detailed view of half of the DST model in isometric perspective

the OGC, the required number of particles was calculated. These particles were generated within the hollow cylinder in the middle of the clay sample. In the next step, the Radius Expansion (RE) method (25) was used to prepare the granular column. During the RE phase, the coefficient of sliding friction between particles was artificially reduced such that the desired relative density was achieved at the end of specimen preparation. Moreover, the degrees of freedom of the platens and mesh nodes during the RE phase were fixed.

After completing the sample preparation stage, all degrees of freedom of mesh nodes, as well as the vertical degrees of freedom of the top and bottom platens, were released. Particles were returned to their original sliding friction coefficients and rolling resistance was activated. The coefficient of friction between OGC and the surrounding clay soil was assumed to be equal to the coefficient of friction between OGC particles. After applying the required normal stress to the top and bottom platens, the computation steps were continued until equilibrium was achieved. Next, during the shearing stage, the bottom and lower side platens were released in the y direction, and a displacement of 3cm was applied to them gradually during 500,000 computational steps. All stages of the test were controlled to ensure that the Index of Unbalanced Force ( $IUF$ ) remained less than 0.01, indicating quasi-static conditions for the sample (25).

### 2. 3. Calibration of Micromaterial Parameters

According to the DEM formulation (Section 2.1), three input parameters ( $k_n$ ,  $\mu$ ,  $\mu_r$ ) are required for a DEM simulation. These parameters were calibrated based on an experimental DST on a soft clay sample improved by a single OGC, which was conducted previously by Aslani, Nazariafshar (8).

The dimensions of the DST test box used in the laboratory experiment were almost the same as those shown in Figure 2. A granular column with a diameter of 169 mm was used. The normal stress in the DST was 55 kPa. It was reported that the friction angle and undrained

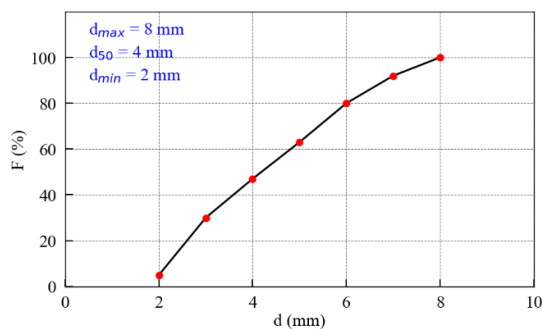


**Figure 2.** Particle Size Distribution (PSD) of soil particles in the OGC

cohesion of soft clay soil were  $\phi = 1^\circ$  and  $c_u = 11 \text{ kPa}$ , respectively.

In the present study, the undrained modulus of elasticity for clay soil was assumed to be  $E_u = 1 \text{ MPa}$ . The assumption was based on a chart proposed by Duncan and Buchignani (26). Accordingly, the ratio between elastic modulus and cohesion of normally consolidated clay soils in undrained conditions ( $E_u/c_u$ ) is expected to fall between 100 and 1500. Due to the very soft nature of the clay soil, this ratio was assumed to be approximately 100 in the present study.

For most granular soils, the interparticle sliding friction coefficient ranges from 0.4 to 0.6, which was assumed to be  $\mu = 0.4$ . A historical match between numerical and experimental curves of shear stress in terms of horizontal displacement was used to determine the values of  $k_n$  and  $\mu_r$ . The value of  $k_n = 100 \text{ kN/m}$  was considered to match the initial slope of these curves at small shear strains (i.e., elastic regime). Assuming  $\mu_r = 0.2$ , the numerical and laboratory shear stress values at the end of the test (i.e., the residual phase) were almost equal. The numerical and experimental curves of shear stress as a function of horizontal displacement are shown in Figure 3. As can be seen, there is a reasonable degree of compatibility between them.

Figure 4 shows the maximum shear strain,  $\gamma_{\max}$ , contour in the clay sample and the Euler-angle,  $\omega$ , contour of the particles in the OGC. As can be seen, particles with high Euler angles and maximum shear strain are concentrated in the shear plane.

### 2. 4. Numerical Tests Program

A parametric study was designed to investigate the effect of various factors including the diameter of the OGC,  $D$ , relative density,  $D_r$ , and sliding,  $\mu$ , and rolling,  $\mu_r$ , friction coefficients between particles of granular soil used in the OGC. The sliding and rolling friction coefficients reflect

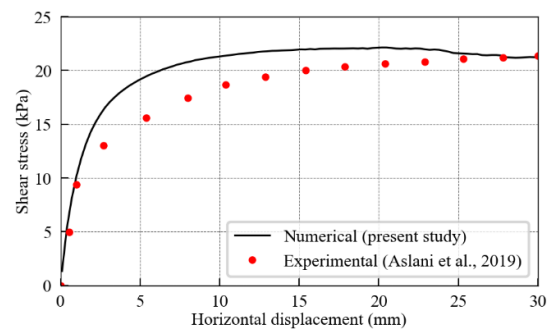


**Figure 3.** Comparison of numerical and experimental curves of shear stress versus horizontal displacement for the DST test

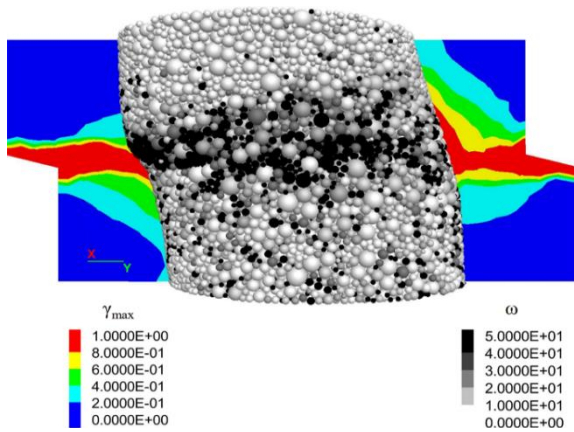


**Figure 4.** Maximum shear strain contour in clayey soil together with Euler-angle contour of particles in the OGC at the end of the test

respectively the roughness of particles and the sphericity and angularity of their shape. An overview of the analyses performed and the entries associated with each analysis can be found in Table 1.

The following points are important to note about Table 1. Each of the T1 to T17 models was subjected to three DST analyses with normal stresses of 50, 100, and 200 kPa according to the methodology described in section 2.2 (a total of 51 analyses). In Table 1,  $A_r$  refers to the area replacement ratio, which is defined as the ratio of the area of the granular column to the area of the test box. It was determined that the artificial interparticle sliding friction coefficients during the RE phase were 0, 0.04, and 0.1, respectively, to reach the relative densities of 100%, 80%, and 60%, respectively. In order to determine the peak and residual friction angles of the granular soils used in the OGC based on their initial relative density,  $D_r$ , and micromaterial parameters,  $\mu$  and  $\mu_r$ , a series of DST tests were performed. Based on those results, the peak,  $\phi_p$ , and residual,  $\phi_{res}$ , friction angles were calculated, which are stated in Table 1. The friction angle and undrained cohesion of soft clay soil were assumed  $\phi = 0$  and  $c_u = 10 \text{ kPa}$ , respectively.

### 3. RESULTS AND DISCUSSION

This section begins with a discussion of the shear behavior of the reference model, model T1. It is then investigated how different parameters, such as the area replacement ratio, the relative density, the roughness, and the shape of soil particles used in OGC, affect the maximum shear strength of clay soil sample improved in the DST test with a single OGC. In the following, we examined the effect of the aforementioned parameters on

**TABLE 1.** An overview of the analyses performed and their associated entries

Model	$D$ (mm)	$A_r$ (%)	$D_r$ (%)	$\mu$	$\mu_r$	$\phi_p$	$\phi_{res}$
T1 to T3	170,	25,					
	130,	15,	80	0.4	0.2	51	34
	200	35					
T4 to T5	170	25	60,	0.4	0.2	48,	34
			100			54	
T6 to T11	170	25	80	0.4	0.2	0.1,	30,
						0.2,	41,
						0.3,	47,
T12 to T17	170	25	80	0.4	0.2	0.5,	53,
						0.6,	55,
						0.8	58
						0,	38,
						0.1,	46,
						0.3,	54,
						0.4,	56,
						0.6,	58,
						0.8	59

the equivalent parameters for the shear strength of soft clay-single OGC composites. Additionally, equivalent parameters obtained from numerical analyses are compared with those obtained from analytical relationships.

#### 3. 1. Preliminary Investigation of Model T1

Figure 5 shows the curves of shear stress in terms of horizontal displacement for the clay-OGC composite and clay at normal stresses of 50, 100 and 200 kPa in model T1. When the normal stress increases, the clay sample retains its maximum shear strength equal to its constant undrained cohesion,  $c_u = 10 \text{ kPa}$ , since its internal friction angle is zero. However, when the normal stress is increased from 50 kPa to 200 kPa, the maximum shear strength of the clay-OGC composite increases from 21 to 45 kPa (more than twice).

In Figure 6, a plot of peak shear stresses versus normal stresses is shown for model T1, on which the Mohr-Coulomb failure line is fitted. The friction angle and cohesion of the clay-OGC composite were determined to be  $9.1^\circ$  and 13.6 kPa, respectively. Therefore, the combination of soft clay soil and a single OGC resulted in not only a significant improvement in friction angle from zero to 9.1, but also a noticeable increase in cohesion from 10 to 13.6 kPa.

**3. 2. Effect of Area Replacement Ratio** Figure 7 illustrates the change in peak shear stress as a function of the area replacement ratio,  $A_r$ . When  $A_r$  is increased from

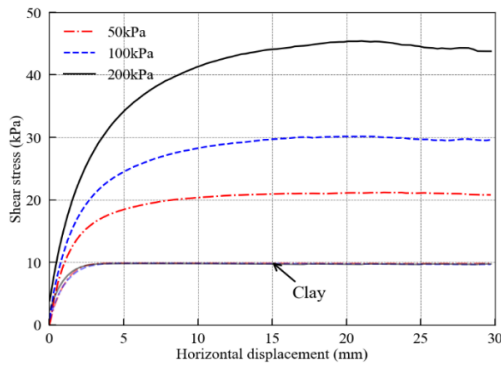


**Figure 5.** Curves of shear stress versus horizontal displacement for the clay-OGC composite and clay at normal stresses of 50, 100 and 200 kPa in the reference model

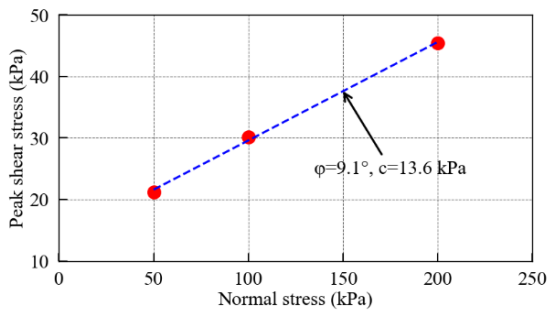


**Figure 6.** The parameters of shear strength, friction angle and cohesion, for the clay-OGC composite in the reference model

15 to 35%, the peak shear stresses for the normal stresses of 50, 100, and 200, respectively increase from 16 to 26 kPa, about 60%, 21 to 39 kPa, about 85%, and 30 to 61 kPa, about 100%. Accordingly, the slope of the increase in the maximum shear strength increases as the normal stress increases.

**3. 3. Effect of Relative Density of OGC** Figure 8 illustrates the peak shear stress as a function of relative density at normal stress levels of 50, 100, and 200 kPa.

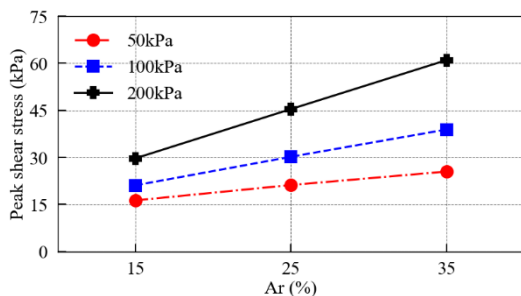


**Figure 7.** Variations of peak shear stress versus area replacement ratio

Increasing  $D_r$  from 60 to 100% results in an increase in peak shear stresses from 20 to 22 kPa, approximately 10%, and from 30 to 32 kPa, approximately 7%, respectively. It is observed that the shear strength remains constant with an increase in  $D_r$  for a normal stress of 200 kPa. As a result, with an increase in  $D_r$ , the shear resistance of the clay-OGC composite is not affected much, and the percentage of changes decreases with an increase in normal stress.

**3. 4. Effect of Roughness of OGC Particles** The coefficient of sliding friction between particles,  $\mu$ , is a measure of particle surface roughness. A plot of peak shear stress versus  $\mu$  is shown in Figure 9. As  $\mu$  increased from 0.1 to 0.8, the peak shear stresses for the normal stresses of 50, 100, and 200 kPa increased respectively from 14 to 23 kPa, about 65%, from 21 to 33 kPa, about 57%, and from 31 to 50 kPa, about 61%. Thus, regardless of the normal stress, an increase in  $\mu$  from 0.1 to 0.8 will result in an increase in peak shear stress of about 60%. Observe that the trend of increasing peak shear stress is not linear so that the slopes of the changes decrease with increasing  $\mu$ .

**3. 5. Effect of Shape of OGC Particles** The coefficient of rolling friction between particles,  $\mu_r$ , is a

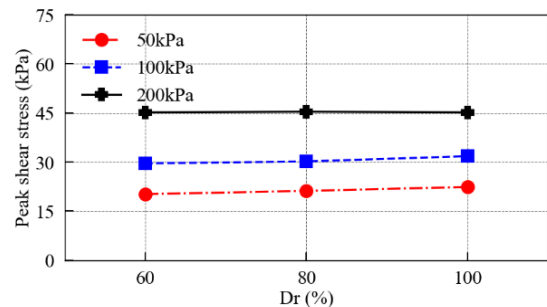


**Figure 8.** Variations of peak shear stress versus relative density

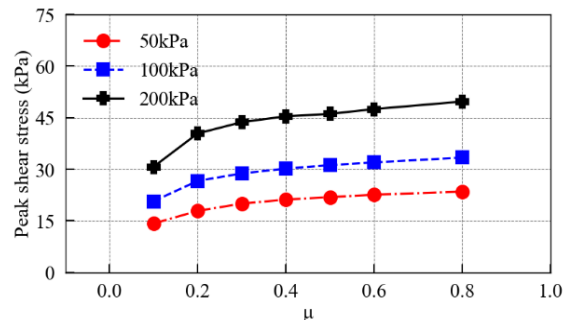


**Figure 9.** Variations in peak shear stress with respect to interparticle sliding friction coefficient

measure of particle shape angularity. The peak shear stress increases with an increase in  $\mu_r$  in a non-linear manner, similar to  $\mu$ . By increasing  $\mu_r$  from 0 to 0.8, the peak shear stresses for normal stresses of 50, 100, and 200 kPa rose from 16 to 24 kPa, approximately 50%, from 23 to 34 kPa, approximately 48%, and from 35 to 52 kPa, approximately 48%, respectively. Therefore, regardless of the normal stress, it can be said that the peak shear stress increases by approximately 50% with an increase of  $\mu_r$  from 0 to 0.8. The coefficient of rolling friction (angularity of the particle shape) appears to have less influence on the shear strength of clay-OGC composites than the coefficient of sliding friction (surface roughness of particles).

**3. 6. Equivalent Shear Strength Parameters** In general, the equivalent shear strength parameters (i.e., cohesion,  $c$ , and friction angle,  $\phi$ ) of a soft clay-OGC composite can be calculated using the area replacement method from Equations 7 and 8.

$$\phi = A_r \phi_s + (1 - A_r) \phi_c \quad (7)$$

$$c = A_r c_s + (1 - A_r) c_c \quad (8)$$

where  $\phi_s$  and  $\phi_c$  refer to the friction angles of the OGC and clay, respectively, and  $c_s$  and  $c_c$  denote their cohesions.

In order to calculate the shear strength equivalent parameters based on the above relationships,  $\phi_c = 0$  and  $c_s = 0$  were assumed. Moreover,  $c_c = c_u = 10$  kPa was taken into account. The equivalent friction angle was calculated once by assuming that the friction angle of the OGC is equal to the peak friction angle of the granular soil,  $\phi_s = \phi_p$ , and once by assuming that the friction angle of the OGC equals the residual friction angle of the granular soil,  $\phi_s = \phi_{res}$ . The values of  $\phi_p$  and  $\phi_{res}$  for the models are presented in Table 1.

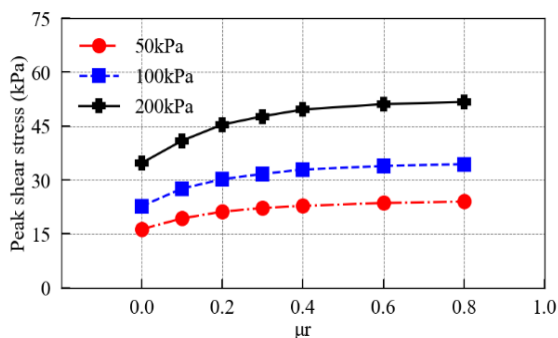


**Figure 10.** Variations in peak shear stress with respect to interparticle rolling friction coefficient

The equivalent friction angle and cohesion obtained from the numerical analysis are termed  $\phi^{Num}$  and  $c^{Num}$ , respectively. They were obtained for each model from a fit similar to that shown for the reference model in Figure 6. The equivalent cohesion calculated from the analytical Equation 8 is referred to as  $c^{Anal}$ . Additionally, the equivalent friction angles calculated from analytical Equation 7 with the assumptions of  $\phi_s = \phi_p$  and  $\phi_s = \phi_{res}$  are referred to as  $\phi_p^{Anal}$  and  $\phi_{res}^{Anal}$ , respectively.

Figures 11 and 12 present the effects of  $A_r$ ,  $D_r$ ,  $\mu$  and  $\mu_r$  on the equivalent friction angle and cohesion, respectively. As  $A_r$  increases from 15% to 35%,  $\phi^{Num}$  and  $c^{Num}$  increase respectively from 5.1° to 13.2° (more than double) and from 12 to 14.5 kPa (nearly 20%). With an increase in  $D_r$  from 60% to 80%,  $\phi^{Num}$  decreases from 9.4° to 8.5° (about 10%), while  $c^{Num}$  increases from 12.4 to 15.6 kPa (about 25%). When  $\mu$  increases from 0.1 to 0.8,  $\phi^{Num}$  and  $c^{Num}$  increase from 6.2° to 9.8° (approximately 60%) and from 9.2 to 15.3 kPa (approximately 66%), respectively. By increasing  $\mu_r$  from 0 to 0.8,  $\phi^{Num}$  and  $c^{Num}$  increase from 7° to 10.4° (about 50%) and from 10.2 to 15.4 kPa (about 86%), respectively.

Figures 11 and 12 illustrate also changes in equivalent friction angle and cohesion,  $\phi_p^{Anal}$ ,  $\phi_{res}^{Anal}$ , and  $c^{Anal}$ , resulting from Equations 7 and 8. It can be seen that the  $\phi^{Num}$  values are very closely matched with the  $\phi_{res}^{Anal}$  values. Therefore, it would be unconservative to calculate the equivalent friction angle using  $\phi_p$  of granular soil. Additionally, a comparison of  $c^{Num}$  and  $c^{Anal}$  values reveals that  $c^{Num}$  values are significantly higher. It is thereby conservative to calculate the equivalent cohesion using Equation 8. All models show that the equivalent cohesion obtained by the numerical analysis is greater than the undrained cohesion of clay soil. As a result of the obtained results, one can say that when calculating the equivalent friction angle for a clay-OGC composite, the residual friction angle,  $\phi_{res}$ , of granular soil should be used rather than its peak friction angle,  $\phi_p$ , in Equation 7. Additionally, the undrained cohesion of clay soil,  $c_u$ , can be used as an equivalent cohesion for the clay-OGC composite.

#### 4. SUMMARY AND CONCLUSION

The present study investigated numerically the shear behavior of soft clay soil improved with one Ordinary Granular Column (OGC) in the Direct Shear Test (DST)

using a combined Discrete Element Method-Finite Difference Method, DEM-FDM. First, a brief description of the methodology and assumptions underlying numerical modeling was provided. By simulating a laboratory DST test, previously performed by Aslani, Nazariafshar (8), and comparing simulated and laboratory shear stress-horizontal displacement curves, the numerical modeling methodology was verified. Afterward, 51 DEM-FDM DST tests were conducted within the framework of a parametric study. We investigated the effect of various macro-scale factors on the shear strength of a soft clay-OGC composite in DST, including the area replacement ratio and the relative density of the granular soil. Furthermore, the effect of various micro-scale factors, including the coefficient of sliding and rolling friction between particles, which represent the roughness

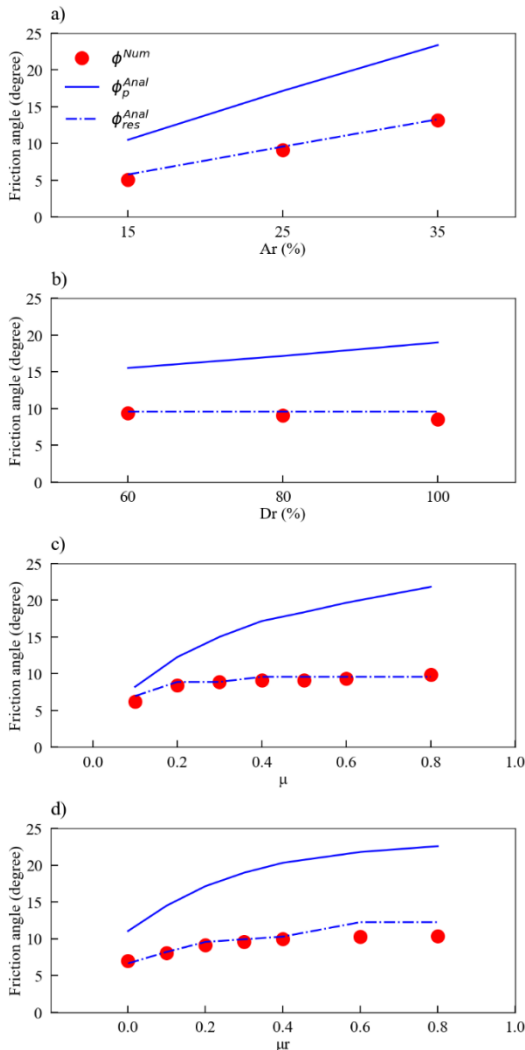


**Figure 11.** Effects of a)  $A_r$ , b)  $D_r$ , c)  $\mu$  and d)  $\mu_r$  on  $\phi^{Num}$ ,  $\phi_p^{Anal}$ , and  $\phi_{res}^{Anal}$

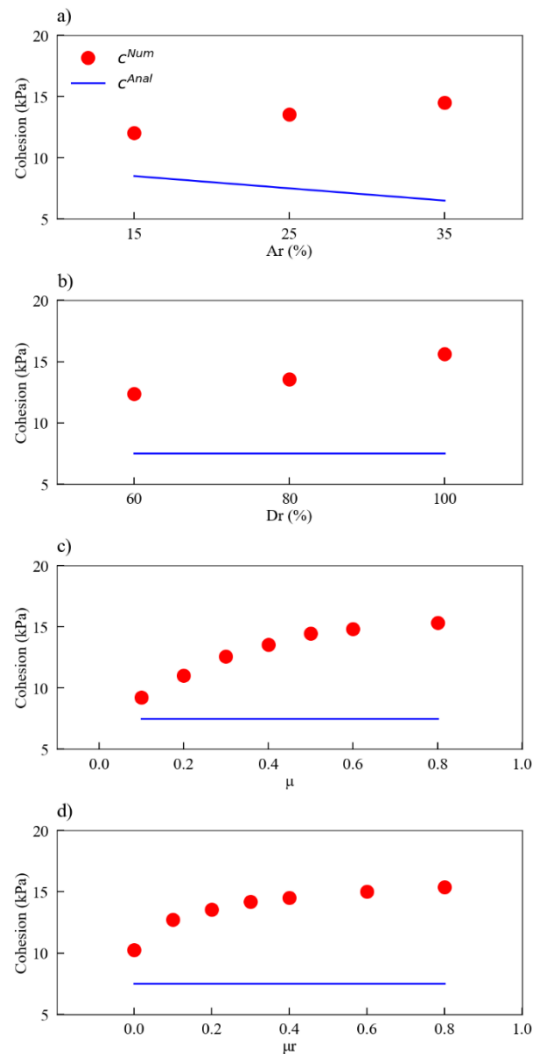


**Figure 12.** Effects of a)  $A_r$ , b)  $D_r$ , c)  $\mu$  and d)  $\mu_r$  on  $c^{Num}$  and  $c^{Anal}$

and angularity of granular soil particles used in OGC, was investigated. Here are some of the most significant results of the present study:

- 1) As the area replacement ratio increased from 15 to 35%, the maximum shear strength of the clay-OGC composite increased by two times, depending on the level of normal stress applied.
- 2) The maximum shear strength of the clay-OGC composite increased by 10% when the relative density of granular soil was increased from 60% to 80%.
- 3) By increasing the interparticle sliding friction coefficient from 0.1 to 0.8, the maximum shear strength of the clay-OGC composite rose by about 60% regardless of the level of normal stress applied. Moreover, it increased by about 50% irrespective of the normal stress when the interparticle rolling



friction coefficient was increased from 0 to 0.8. Thus, it can be concluded that the surface roughness of granular soil particles used in OGC has a greater impact on the composite shear strength than their angularity.

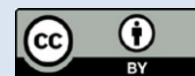
- 4) It was found that the equivalent friction angles calculated from the numerical analysis for the clay-OGC composite were very similar to the ones determined by the area replacement method based on the residual friction angle of the granular soil. Furthermore, the equivalent cohesions obtained from the numerical analysis were greater than the undrained cohesion of clay soil. As a consequence, it may be recommended to determine the equivalent friction angle of clay-OGC composites by using the residual friction angle of granular soil and the area replacement method. Moreover, the undrained cohesion of clay soil can be considered as an equivalent cohesion for clay-OGC composites.

## 5. REFERENCES

- Shahmandi A, Ghazavi M, Barkhordari K, Hashemi M. The Effect of Using Reinforced Granular Blanket and Single Stone Column on Improvement of Sandy Soil: Experimental Study. *Int J Eng.* 2023;36(8):1532-47. 10.5829/ije.2023.36.08b.13
- Murugesan S, Rajagopal K. Geosynthetic-encased stone columns: numerical evaluation. *Geotext Geomembr.* 2006;24(6):349-58. 10.1016/j.geotexmem.2006.05.001
- Yoo C, Kim S-B. Numerical modeling of geosynthetic-encased stone column-reinforced ground. *Geosynth Int.* 2009;16(3):116-26. 10.1680/gein.2009.16.3.116
- Khabbazian M, Kaliakin VN, Meehan CL. Numerical study of the effect of geosynthetic encasement on the behaviour of granular columns. *Geosynth Int.* 2010;17(3):132-43. 10.1680/gein.2010.17.3.132
- Abdelhamid M, Ali N, Abdelaziz T. A Literature Review of Factors Affecting the Behavior of Encased Stone Columns. *Geotech Geol Eng.* 2023;41(6):3253-88. 10.1007/s10706-023-02492-8
- Mazumder T, Rolaniya AK, Ayothiraman R. Experimental study on behaviour of encased stone column with tyre chips as aggregates. *Geosynth Int.* 2018;25(3):259-70. 10.1680/jgein.18.00006
- Mohapatra SR, Rajagopal K, Sharma J. Direct shear tests on geosynthetic-encased granular columns. *Geotext Geomembr.* 2016;44(3):396-405. 10.1016/j.geotexmem.2016.01.002
- Aslani M, Nazariafshar J, Ganjian N. Experimental Study on Shear Strength of Cohesive Soils Reinforced with Stone Columns. *Geotech Geol Eng.* 2019;37(3):2165-88. 10.1007/s10706-018-0752-z
- Murugesan S, Rajagopal K. Shear Load Tests on Stone Columns With and Without Geosynthetic Encasement. *Geotech Test J.* 2009;32(1):76-85. 10.1520/GTJ101219
- Shehata H, Sorour T, Fayed A. Effect of stone column installation on soft clay behavior. *International Journal of Geotechnical Engineering.* 2018. 10.1080/19386362.2018.1478245
- Mohanty P, Samanta M. Experimental and numerical studies on response of the stone column in layered soil. *Int J Geosynth Ground Eng.* 2015;1:1-14. 10.1007/s40891-015-0029-z
- Basack S, Indraratna B, Rujikiatkamjorn C. Modeling the performance of stone column-reinforced soft ground under static and cyclic loads. *J Geotech Geoenviron Eng.* 2016;142(2):04015067. 10.1061/(ASCE)GT.1943-5606.0001378
- Schweiger H, Pande G. Numerical analysis of stone column supported foundations. *Comput Geotech.* 1986;2(6):347-72. 10.1016/0266-352X(86)90030-3
- Gholaminejad A, Mahboubi A, Noorzad A. Hybrid Continuous-Discrete Modeling of an Ordinary Stone Column and Micromechanical Investigations. *Geotech Geol Eng.* 2021;39(4):3249-64. 10.1007/s10706-021-01692-4
- Indraratna B, Ngo NT, Rujikiatkamjorn C, Sloan SW. Coupled discrete element-finite difference method for analysing the load-deformation behaviour of a single stone column in soft soil. *Comput Geotech.* 2015;63:267-78. 10.1016/j.compgeo.2014.10.002
- Tan X, Feng LJ, Hu ZB, Abbas SM. The equivalent shear strength properties of the composite soil reinforced by stone columns: an FDM-DEM-coupled numerical evaluation. *Environ Earth Sci.* 2021;80(4):12. 10.1007/s12665-021-09412-0
- Tan X, Feng LJ, Hu ZB, Zhao MH. A DEM-FDM coupled numerical study on the deformation and failure process of the isolated stone column in soft soil. *Bull Eng Geol Environ.* 2020;79(4):1693-705. 10.1007/s10064-019-01671-3
- Tan X, Zhao MH, Chen W. Numerical Simulation of a Single Stone Column in Soft Clay Using the Discrete-Element Method. *Int J Geomech.* 2018;18(12):12. 10.1061/(asce)gm.1943-5622.0001308
- Mohapatra SR, Rajagopal K, Sharma J. 3-Dimensional numerical modeling of geosynthetic-encased granular columns. *Geotext Geomembr.* 2017;45(3):131-41. 10.1016/j.geotexmem.2017.01.004
- Cundall PA, Strack OD. A discrete numerical model for granular assemblies. *geotechnique.* 1979;29(1):47-65. 10.1680/geot.1979.29.1.47
- Itasca. PFC3D manual, Version 6.0. 2016.
- Yan Y, Ji S. Discrete element modeling of direct shear tests for a granular material. *Int J Numer Anal Methods Geomech.* 2010;34(9):978-90. 10.1002/nag.848
- Potts D, Dounias G, Vaughan P. Finite element analysis of the direct shear box test. *Geotechnique.* 1987;37(1):11-23. 10.1680/geot.1987.37.1.11
- Yunjia W, Erxiang S. Discrete element analysis of the particle shape effect on packing density and strength of rockfills. *Rock and Soil Mechanics.* 2019;40(6):2416-26.
- O'Sullivan C. Particulate discrete element modelling: a geomechanics perspective: CRC Press; 2011.
- Duncan JM, Buchignani A. An Engineering Manual for Settlement Studies: By JM Duncan and AL Buchignani: Department of Civil Engineering, University of California; 1976.

**COPYRIGHTS**

©2024 The author(s). This is an open access article distributed under the terms of the Creative Commons Attribution (CC BY 4.0), which permits unrestricted use, distribution, and reproduction in any medium, as long as the original authors and source are cited. No permission is required from the authors or the publishers.

**Persian Abstract****چکیده**

تحقیقات زیادی در مورد عملکرد ستون‌های دانه‌ای تحت بارهای عمودی انجام شده است. اما در برخی شرایط، حرکت توده خاک می‌تواند منجر به تغییر شکل‌های جانبی و در نتیجه تنش‌های برشی در خاک و ستون‌ها شود. هدف اصلی مطالعه حاضر، بررسی عددی عملکرد برشی خاک رسی نرم بهبودیافته با یک ستون دانه‌ای معمولی (OGC) در آزمایش برش مستقیم با استفاده از روش ترکیبی اجزای مجزا - تفاضل محدود (DEM-FDM) است. روش مدل‌سازی عددی ابتدا با شبیه‌سازی یک آزمایش برش مستقیم که قبلاً روی یک کامپوزیت خاک رس نرم-OGC در آزمایشگاه انجام شده بود صحت‌سنجی شد. پس از آن، یک مطالعه پارامتری گسترده برای تعیین اینکه چگونه عوامل مختلف بر استحکام برشی کامپوزیت‌های رس-OGC تأثیر می‌گذارند، انجام شد. با توجه به نتایج، افزایش نسبت جایگزینی سطح از ۱۵ به ۳۵ درصد می‌تواند حداکثر مقاومت برشی کامپوزیت‌های رس-OGC در آزمایش برش مستقیم را بسته به سطح تنش نرمال اعمال شده تا دو برابر افزایش دهد. نتایج مقیاس میکرو همچنین نشان داد که زبری سطح ذرات خاک دانه‌ای در OGC تأثیر بیشتری بر مقاومت برشی کامپوزیت‌های رس-OGC نسبت به زاویه‌دار بودن شکل آنها دارد. علاوه بر این، نتایج نشان داد که زاویه اصطکاک معادل کامپوزیت‌های رس-OGC باید بر اساس زاویه اصطکاک باقیمانده خاک دانه‌ای مورد استفاده در OGC محاسبه شود.